April 1992 • NREL/TP-413-4835

Development of a Computer Model for Polycrystalline Thin-Film $CuInSe_2$ and CdTe Solar Cells

Annual Subcontract Report 1 January 1990 - 31 December 1990

J. L. Gray
R. J. Schwartz
Y. J. Lee
Purdue University
West Lafayette, Indiana

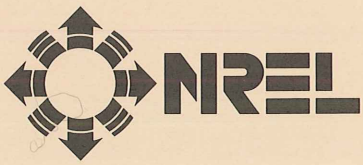

National Renewable Energy Laboratory
A Division of Midwest Research Institute
Operated for the U.S. Department of Energy
Under Contract No. DE-AC02-83CH10093

NREL/TP-413-4835 • UC Category: 273 • DE92001242

Development of a Computer Model for Polycrystalline Thin-Film $CuInSe_2$ and CdTe Solar Cells

Annual Subcontract Report 1 January 1990 - 31 December 1990

NREL/TP--413-4835

DE92 001242

J. L. Gray
R. J. Schwartz
Y. J. Lee
Purdue University
West Lafayette, Indiana

NREL technical monitor: H. S. Ullal

National Renewable Energy Laboratory
(formerly the Solar Energy Research Institute)
1617 Cole Boulevard
Golden, Colorado 80401-3393
A Division of Midwest Research Institute
Operated for the U.S. Department of Energy
under Contract No. DE-AC02-83CH10093

Prepared under Subcontract No. XN-0-10013-1

April 1992

On September 16, 1991 the Solar Energy Institute was designated a national laboratory, and its name was changed to the National Renewable Energy Laboratory.

Printed in the United States of America
Available from:
National Technical Information Service
U.S. Department of Commerce
5285 Port Royal Road
Springfield, VA 22161

Price: Microfiche A01
Printed Copy A03

Codes are used for pricing all publications. The code is determined by the number of pages in the publication. Information pertaining to the pricing codes can be found in the current issue of the following publications which are generally available in most libraries: *Energy Research Abstracts (ERA)*; *Government Reports Announcements* and Index (*GRA* and I); *Scientific and Technical Abstract Reports (STAR)*; and publication NTIS-PR-360 available from NTIS at the above address.

Table of Contents

1. Introduction

1.1. Project Overview

The purpose of this work is to develop a highly accurate numerical model for $CuInSe_2$ and CdTe solar cells. ADEPT (A Device Emulation Program and Toolbox), a one-dimensional semiconductor device simulation code developed at Purdue University, is being used as the basis of this model. An additional objective is to use ADEPT to analyze the performance of existing and proposed $CuInSe_2$ and CdTe solar cell structures.

This work is being performed in two phases. The first phase involved collecting device performance parameters, cell structure information, and material parameters. This information was used to construct the basic models needed by ADEPT to simulate $CuInSe_2$ and CdTe solar cells. This report is a summary of the information gathered during the first phase. The second phase will entail further development and release of a version of ADEPT, tailored to $CuInSe_2$ and CdTe solar cells, which can be run on a personal computer. In addition, ADEPT will be used to analyze the performance of existing and proposed $CuInSe_2$ and CdTe solar cell structures.

1.2. Scope of This Report

This report is a tabulation of information gathered during the first phase of this project on the performance of existing $CuInSe_2$ and CdTe solar cells, the material properties of $CuInSe_2$, CdTe, and CdS, and the optical absorption properties of $CuInSe_2$, CdTe, and CdS. This is the basic information needed to begin development of an accurate numerical model of $CuInSe_2$ and CdTe solar cells.

2. Survey of $CuInSe_2$ Solar Cells

2.1. Measured Solar Cell Parameters

$CuInSe_2$ has for some time been considered a good candadate material for inexpensive and relatively efficient solar cells. It has a high absorption coefficient and is inexpensive. Many techniques for making the material have been developed and various solar cell structures have been tested, resulting in a steady increase in the $CuInSe_2$ based solar cell efficiency. Also, $CuInSe_2$ solar cells fabricated to date have demonstrated excellent stability.

The highest $CuInSe_2$ cell efficiency to date is 14.1 % for a ZnO/thin - CdS/CIS cell. For this cell, Jsc was 41.0 mA/cm^2 and Voc was 0.508 V with fill factor of 0.677 under 100 mW/cm^2 ASTM Air Mass 1.5 global spectrum.

Table 2.1 shows the measured performance of some $CuInSe_2$ solar cells. Figure 2.1 to 2.4 are various plots of the performance of $CuInSe_2$ solar cells. These figures show a wide range in cell performance. Figure 2.1 is the plot of Voc vs efficiency. It is noticeable that cells with high open circuit voltages generally have high efficiencies. Although solar cells with CdS or ZnO for window layers do not have high open circuit voltages, those ones fabricated with ZnO/CdS as window layers display the best open circuit voltages. Jsc vs efficiency is plotted in figure 2.2. (Figure 2.2 (a) is the plot of short circuit current vs efficiency of the cells with different window materials. Figure 2.2 (b) shows the same plot but indicates the illumination intensity at which the cells were measured.) It is apparent that the solar cell performances in this plot are scattered over a wide range and there seems to be little relation between short circuit current, efficiency and the type of material used for window. In figure 2.3 of fill factor vs efficiency, it can be seen that solar cells with high fill factors also have high efficiencies. Solar cells with (CdZn)S:In, (CdZn)S and ZnO/CdS have high fill factors, so high efficiencies. Figure 2.4 shows a plot of Voc vs Jsc. No relation between open circuit voltage and short circuit current could be found, especially in the cells with ZnO/CdS window layers which possessed the highest efficiencies.

Table 2.1 Survey of Measured $CuInSe_2$ Cells

window	Voc [V]	Jsc [mA/cm^2]	FF	Efficiency. [%]	Illumination	Ref.
CdS	0.396	35	0.64	8.72	AM1	[13]
	0.396	39	0.63	9.53* (10.01**)	ELH	
	0.380	35	0.63	8.95	sun 93.9 mW/cm^2	
	0.3	34	0.44	6.9	ELH 60 mW/cm^2	[35]
	0.470	30.50	0.715	10.26* (10.8**)		[38]
	~ 0.43	~ 32	~0.67		AM1	[24]
	0.42	35 - 40	0.66			[18]
bi - layer	0.370	35	0.64	8.5		[34]
	0.395	38	0.67	10.1		
	0.397	36	0.53	7.7\9.9		
	0.44	34		9.9		
single-layer	0.278	36	0.55	5.5		
	0.44	35.6	0.62	9.7	100 mW/cm^2	[7]
	0.35	31.7	0.38	4.2	AM1.5	
	0.396	39	0.63	9.53	AM1	[37]
					101.5 mW/cm^2	
(CdZn)S:In	0.418	36.6	0.689	10.5	100 mW/cm^2	[30]
	0.400	38.4	0.66	10.1	AM1.5	
	0.425	35.9	0.685	10.4		
	0.419	36.6	0.634	9.7		
(CdZn)S	0.430	37.0	0.675	12.3	ELH	[5]
	0.433	35.2	0.66	11.5	87.5 mW/cm^2	
	0.430	34.4	0.686	11.3		
	0.429	32.2	0.666	10.5		
	0.428	32.4	0.664	10.5		
	0.43	39			ELH 87.5mW/cm^2	[12]
					normalized to 100	
	0.404	36.1	0.677	9.9	ELH , normalized	[39]
					to AM1.5	
	0.4	32.5	0.647	9.64	87.5 mW/cm^2	[28]

Table 2.1 continued

window	Voc [V]	Jsc [mA/cm2]	FF	Efficiency. [%]	Illumination	Ref.
ZnO	0.22	39.8	0.47	4.0	ELH 87.5 mW/cm^2, normalized to 100 mW/cm^2,	[30]
	0.463	26.52	0.666	8.18* (10.89**)		[38]
ZnCdS	0.4314	38.96	0.6309	10.6	ELH 100 mW/cm^2	[37]
ZnO/thin-CdS	0.487	32.85	0.7	11.2* (12.5 **)	Spectrolab XT-10 AM1.5 global 100 mW/cm^2	[21]
	0.455	40.6	0.661	12.2	100mW/cm^2 AM1.5 global	[15]
	0.445	34.7	0.596	9.19	100 mW/cm^2, ASTM AM 1.5 global	[20]
	0.508	41.0	0.677	14.1 **	XT-10 100 mW/cm^2, AM1.5	[14] [40]

** Efficiencies with ** are the active area efficiencies.

* Efficiencies with * are the total efficiencies.

All the others do not specify which efficiency they were measuring.

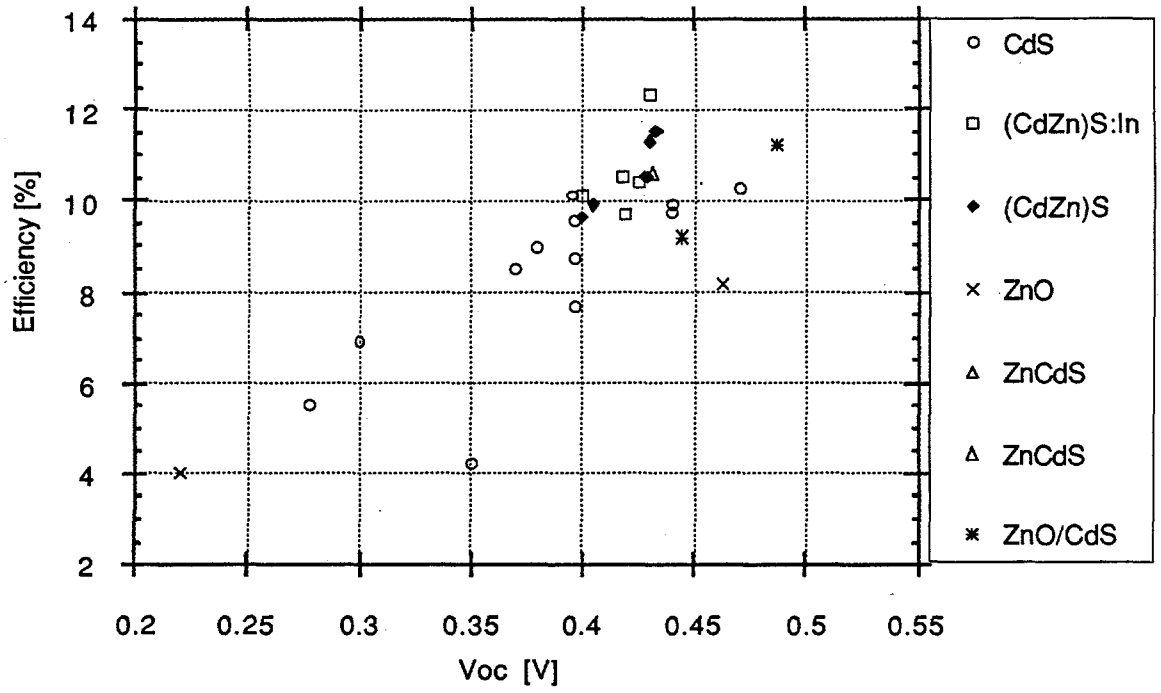

Figure 2.1 The open circuit voltage vs efficiency of surveyed cell performance is plotted. The cells with different window layers are indicated with the symbols.

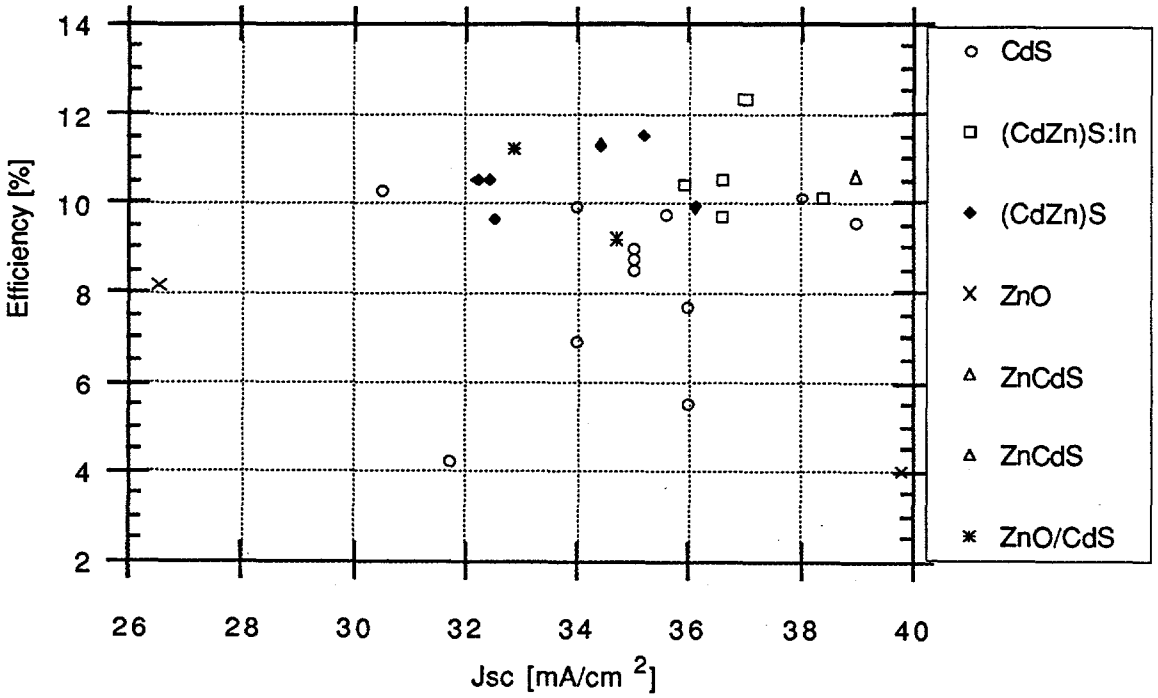

Figure 2.2 (a) Short circuit current vs efficiency of surveyed CIS cell performance.

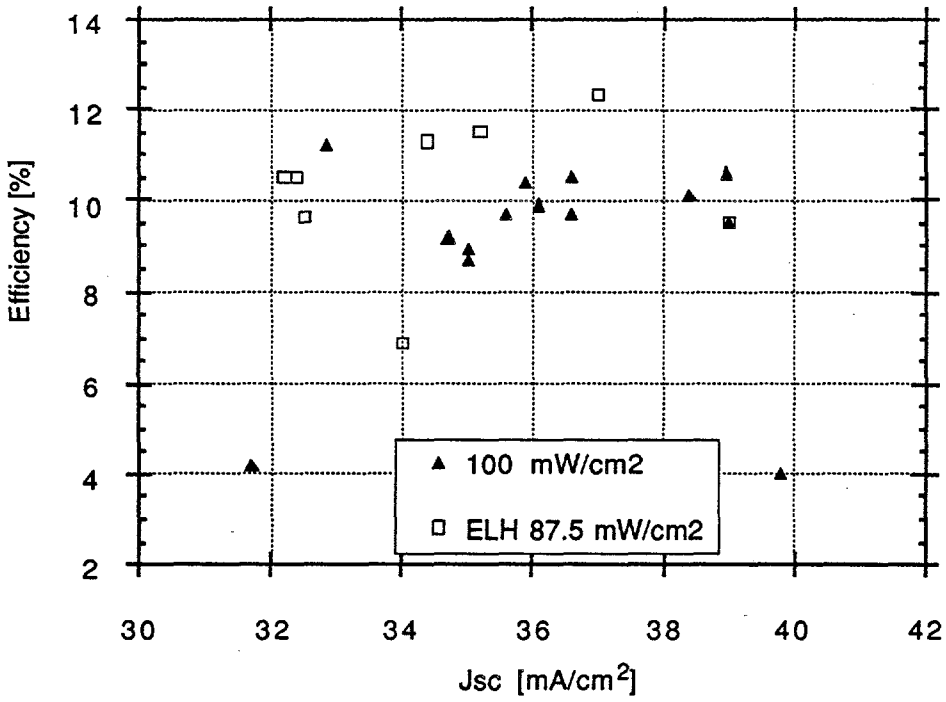

Figure 2.2 (b) Short circuit current vs efficiency of surveyed CIS cell performance. The intensity of the illumination is indicated.

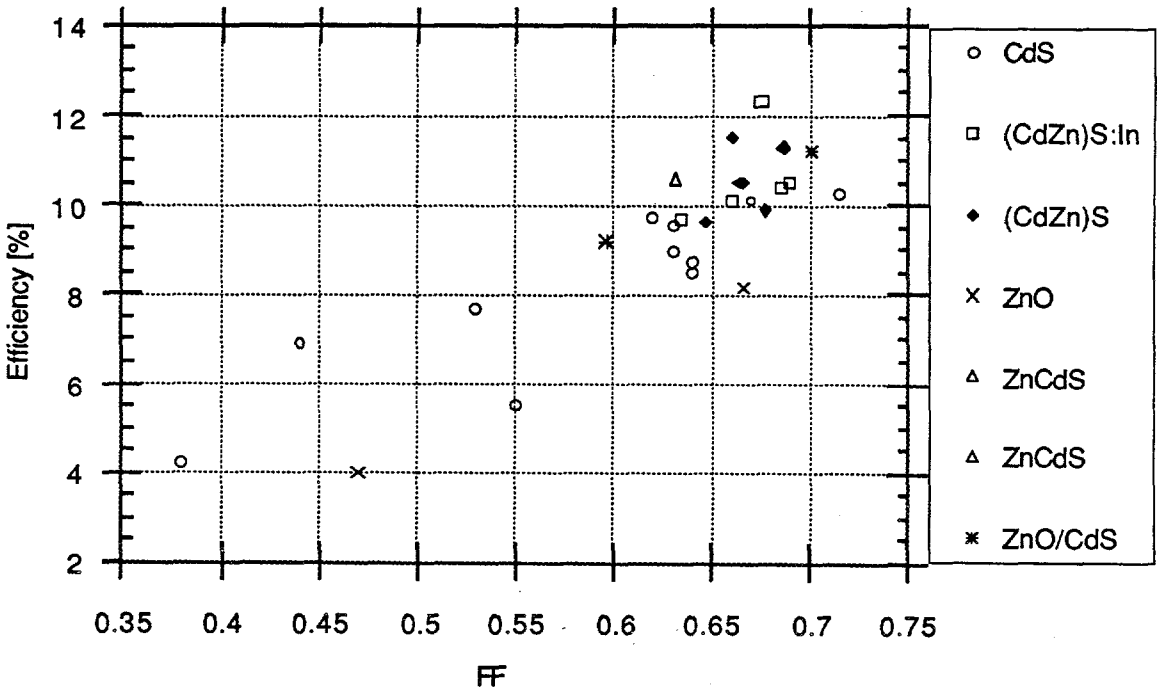

Figure 2.3 Fill factor vs efficiency of surveyed CIS cells.

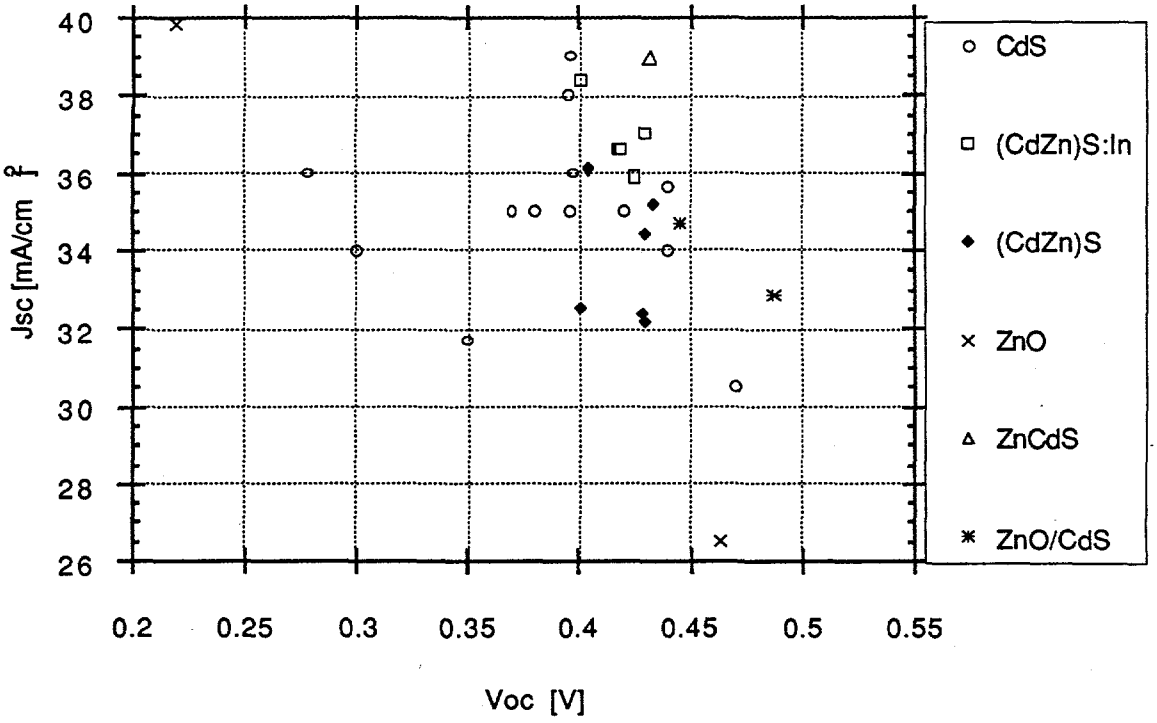

Figure 2.4 Open circuit voltage vs short circuit current of surveyed CIS cells.

2.2. Material Properties

Most of the $CuInSe_2$ cells have a very high short circuit current but only a moderate open circuit voltage and fill factor. To have an insight of what the dominant current transport mechanism is and which structure yields the best efficiency, etc., numerical modeling of these $CuInSe_2$ cells is required.

In order to model the CIS solar cells accurately, it is extremely important to enter the correct values of material parameters. These parameters are found from numerous literatures. When there is discrepancy, the most common and/or average values are used. For CIS the mobilities and defect levels are very much scattered depending on the method of material growth and after treatments. The bulk properties of $CuInSe_2$ are shown in Table 2.2. Although there are some basic values for band gap energy, dielectric const and lattice constant, the values of mobility of carriers and electron affinity vary very much. These parameter values differ depending on the methods and technologies of fabrication of the material. Numerical modelling of $CuInSe_2$ solar cells could determine the most likely parameter values for this material.

Table 2.2 $CuInSe_2$ Material Parameters

	values	reference	values used
Eg [eV]	0.95- 1.01	[27][33]	1.00
	1.04	[31]	
	1.94 -1.06	[36]	
	1.0	[23]	
	1.01 - 1.03	[16]	
	1.15	[8]	
	1.1	[29]	
	1.02	[9][10]	
Hall mobility $[cm^2/V/s]$	$\mu p = 2.8$	[11]	
	$\mu n = 1.4$		
	$\mu p = 8.08$	[29]	
	$\mu n = 23.8$	[35]	

Table 2.2 continued

	values	reference	values used
mobility [$cm^2/V/s$]	63 - 485	[36]	$\mu_n = 50$
	> 500		$\mu_p = 5$
	15 - 50	[17]	
	10 - 27	[26]	
	5 - 150	[2]	
	2 (p-type)	[10]	
	4 (n-type)		
	20 (hole)	[1]	
electron affinity [eV]	5.48	[31]	4.3
	4.3	[16][25]	
dielectric constant	eo=13.6 ea=8.1	[36] [4]	13.5
	eo=15.2 e =8.5	[22]	
	eo=16.0 e =9.5		
refraction index	2.90	[32]	
	2.79	[3]	
reflection coefficient	0.257	[3]	
Nc [$/cm^3$]	6.6e17	[3]	6.6e17
	5.0e18	[2]	
Nv [$/cm^3$]	1.5e19	[3]	1.5e19
	1.0e19	[2]	
carrier life time [nsec]	10 - 190	[25]	10
lattice constant [Å]	a = 5.782 c = 11.62	[31]	
	a = 5.785 c/a = 2	[19]	
effective mass	$m_n^* = 0.09\ m_o$	[6]	
	$m_h^* = 0.73\ m_o$		
	$m_{hh} = 0.71\ m_o$	[25]	
	$m_{lh} = 0.092 m_o$		

2.3. List of References for CIS

1. B. Tell, S. Wagner, and P. M. Bridenbaugh, "Motion of p-n Junctions in $CuInSe_2$," Applied Physics Letters, Vol.28, no.8, p.454, 1976.

2. K. W. Boer, "Polycrystalline Semiconductor Heterojunction Modeling ($CdS/CuInSe_2$)," Solar Cells, Vol.16, pp.591-609, 1989.

3. D. Cahen, "Survey of Literature Results: Electronic, Electrical,Thermal and Further Properties of $CuInSe_2$," 1985.

4. N. Christoforou, J. D. Leslie, and S. Damaskinos, "Study of Deep Levels in $CuInSe_2$ by Deep Level Transient Spectroscopy Measurements on $CdS/CuInSe_2$ Solar Cells," Solar Cells, Vol.26, pp.197-214, 1989.

5. S. Damaskinos, J. E. Phillips, M. Roy, and R. W. Birkmire, "High Efficiency $CuInSe_2$-(CdZn)S Solar Cells: Fabrication, Results, and Analysis," Canadian Journal of Physics, Vol.67, pp.420-424, 1989.

6. W. E. Devaney, R. A. Mickelsen, and W. S. Chen, "Recent Improvement in $CuInSe_2$/ZnCdS Thin Film Solar Cell Efficiency," 18th IEEE Photovoltaic Specialists Conference, p.1733, 1985.

7. C. Eberspacher, B. Felder, R. R. Potter, R. D. Wieting, "Design and Fabrication of Thin Film Si:H/Copper Indium Diselenide Tandem Modules," 18th IEEE Photovoltaic Specialists Conference, p.1031, 1985.

8. J. C. Garg, R. P. Sharma, and K. C. Sharma, "Characterization of p-$CuInSe_2$ Films for Photovoltaics Grown by a Chemical Deposition Technique," Thin Solid Films, Vol.164, pp.269-273, 1988.

9. B. Haba, C. W. Bates,Jr., B. J. Brown, and Z. Ndlela, "Characterization of Structural Defects in the Presence of In_2O_3 in CuInSe2 Prepared by Spray Pyrolysis," Solar Cells, Vol.28, pp.177-183, 1990.

10. D. Haneman, S. N. Sahu, and R. D. L. Kristensen, "$CuInSe_2$ Films for Photovoltaics and Photoelectrochemistry," Thin Solid Films, Vol.163, pp.167-174, 1988.

11. S. Isomura, H. Hayashi, and S. Shirakata, "Observation of the Growth Process of $CuInSe_2$ Thin Films," Solar Energy Materials, Vol.18, pp.179-189, 1989.

12. B. E. McCandless, and R. W. Birkmire, "Control of Deposition and Surface Properties of $CuInSe_2$ Thin Films for Solar Cells," 20th IEEE Photovoltaic Specialists Conference, p.1510, 1988.

13. R. A. Mickelsen, and W. S. Chen, "Development of 9.4% Efficient Thin-Film $CuInSe_2$/CdS Solar Cell," 15th IEEE Photovoltaic Specialists Conference, p.800, 1981.

14. K. Mitchell, C. Eberspacher, J. Ermer, and D. Pier, "Single and Tandem Junction $CuInSe_2$ Cell and Module Technology," 20th IEEE Photovoltaic Specialists Conference, pp.1384-1389, 1988.

15. K. W. Mitchell, and H. I. Liu, "Device Analysis of $CuInSe_2$ Solar Cells," 20th IEEE Photovoltaic Specialists Conference, p.1461, 1988.

16. H. Neumann, "Optical Properties and Electronic Band Structure of $CuInSe_2$," Solar Cells, Vol.16, pp.317-333, 1986.

17. H. Neumann, and R. D. Tomlinson, "Relation between Electrical Properties and Composotion in $CuInSe_2$ Single Crystals," Solar Cells, Vol.28, pp.301-313, 1990.

18. R. Noufi, V. Ramanathan, and R. J. Matson, "Low-Temperature Characteristics of $CdS/CuInSe_2$ Diodes," Solar Cells, Vol.24, pp.11-17, 1988.

19. J. Parkes, R. D. Tomlinson and M. J. Hampshire, "Crystal Data for $CuInSe_2$," Journal of Applied Crystallography, Vol.6, p.414, 1973.

20. R. R. Potter, "Enhanced Photocurrent $ZnO/CdS/CuInSe_2$ Solar Cells," Solar Cells, Vol.16, pp.521-527, 1986.

21. R. R. Potter, C. Eberspacher, and L. B. Fabick, "Device Analysis of $CuInSe_2$/(Cd,Zn)S/ZnO Solar Cells," 18th IEEE Photovoltaic Specialists Conference, p.1695, 1985.

22. V. Riede, H. Sobotta, H. Neumann, H. X. Nguyen, W. Moller, and G. Kuhn, "Infrared Lattice Vibration Spectra of $CuInSe_2$ and $CuGaTe_2$," Solid State Communications, Vol.28, pp.449-454, 1978.

23. C. Rincon, C. Bellabarba, J. Gonzalez, and G. S. Perez, "Optical Properties and Characterization of $CuInSe_2$," Solar Cells, Vol.16, pp.335-349, 1986.

24. V. Ramanathan, R. Noufi, and R. C. Powell, "Defect Levels in $CdS/CuInSe_2$ Thin-Film Solar Cells," Journal of Applied Physics, Vol.63, no.4, p.1203, 1988.

25. C. Goradia, amd M. Ghalla-Goradia, "Theory of High Efficient (Cd,Zn)S/$CuInSe_2$ Thin Film Solar Cells," Solar Cells, vol.16, pp.611-630, 1986.

26. A. Rothearf, "$CuInSe_2$/CdS - Modeling and Analysis," 18th IEEE Photovoltaic Specialists Conference, p.1423, 1985.

27. A. Rothwarf, "$CuInSe_2$/Cd(Zn)S Solar Cell Modeling and Analysis," Solar Cells, Vol.16, pp.567-590, 1986.

28. M. Roy, S. Damaskinos, and J. E. Phillips, "The Diode Current Mechanism in $CuInSe_2$/(CdZn)S Heterojunctions," 20th IEEE Photovoltaic Specialists Conference, p.1618, 1988.

29. S. N. Sahu, R. D. L. Kristensen, and D. Haneman, "Electrodeposition of $CuInSe_2$ Thin Films from Aqueous Solution," Solar Energy Materials, Vol.18 pp.385-397, 1989.

30. W. N. Shafarman, and R. W. Birkmire, "Characterization of Window Layers in $CuInSe_2$ Thin-Film Solar Cells," 20th IEEE Photovoltaic Specialists Conference, p.1515, 1988.

31. R. Trykozko, R. Bacewicz, and J. Filipowicz, "Photoelectrical Properties of $CuInSe_2$ Thin Films," Solar Cells, Vol.16, pp.351-356, 1986.

32. J. R. Tuttle, D. Albin, R. J. Matson, and R. Noufi, "A Comprehensive Study on the Optical Properties of Thin-Film $CuInSe_2$ as a Fuction of Composition and Substrate Temperature".

33. J. R. Tuttle, R. Noufi, R. G. Dhere, C. Kennedy, R. Matson, J. Dolan, J. goral, "Optical Properties of $CuInSe_2$ Thin Films," SERI Polycrystalline Thin Film Program Meeting, 1987.

34. J. R. Tuttle, M. Ruth, D. Albin, A. Matson, and R. Noufi, "Experiments on the Modification of the Bi-Layer Structure in $CdS/CuInSe_2$ Devices," 20th IEEE Photovoltaic Specialists Conference, p.1525, 1988.

35. O. Vigil, abd D. Seuret, "Sintered p-$CuInSe_2$/N-CdS Photovoltaic Heterojunction," Materials Letters, Vol.16, No.3, p.85, 1987.

36. S. M. Wasim, "Transport Properties of $CuInSe_2$," Solar Cells, Vol.16, pp.289-316, 1986.

37. R. A. Mickelsen, and W. S. Chen, "Polycrystalline Thin-Film $CuInSe_2$ Solar Cells," 16th IEEE Photovoltaic Specialists Conference, p.781, 1982.

38. B. M. Masol, and V. K. Kapur, "$CuInSe_2$ Thin Films and High-Efficiency Solar Cells Obtained by Selenization of Metallic Layers," 21st IEEE Photovoltaic Specialists Conference, p.546, 1990.

39. W. N. Shafarman, R. W. Birkmire, D. A. Fardig, B. E. McCandless, A. Mondal, J. E. Phillips and R. D. Varrin,Jr., "Advances in $CuInSe_2$ and CdTe Thin Film Solar Cells," Solar Cells, Vol.30, pp.61-67, 1991.

40. K. W. Mitchell, W. Chesarek, D. R. Willett, C. Eberspacher, J. H. Ermer and R. R. Gay, "$CuInSe_2$ Photovoltaic Modules," Solar Cells, Vol.30, pp.131-136, 1991.

3. Survey of CdTe Solar Cells

3.1. Measured Solar Cell Parameters

Cadmium Telluride is a promising material for solar cells. It has a band gap energy which is near an ideal band gap energy for solar cells. Like CIS, the performance of CdTe based solar cells are improving.Cadmium Telluride based solar cells have higher open circuit voltages than $CuInSe_2$ cells as expected since CdTe has larger band gap, but the short circuit currents and fill factors are not as good. Recently, many CdTe solar cells with efficiencies greater than 10 % have been reported. The best one is Schoktty diode fabricated with Au. The efficiency of this cell was 15.1 % but only one literature on the cells with Au could be found.[49] The next best cell fabricated so far has an efficiency of 13.4 %. The performance of a variety of CdTe solar cells is summarized in Table 3.1. These data are plotted in figure 3.1 to 3.3. Figure 3.1 shows the plot of Voc vs efficiency. Ignoring the one with Au, CdS/CdTe solar cells seem to have the best open circuit voltage and efficiency. The open circuit voltage and efficiency of ITO/CdTe cells are widely scattered. As expected solar cells with high open circuit voltage have high efficiency. Figure 3.2 is the plot of Jsc vs efficiency. A cluster is found in the ranges of 20 to 25 mA of short circuit current and 10 to 12 % of efficiency, regardless of which type of window layer materials are used. It is interesting that CdTe solar cells with highest Jsc fabricated to date do not have the highest efficiencies. However, the general trend is that cells with high short circuit current exhibit high efficiencies. Fill factor vs efficiency for CdTe solar cells is plotted in figure 3.3. This plot shows scattered data over a wide range. Solar cells with high fill factor do not necessarily have high efficiency. Even in cells with the same window materials, any consistency could not be determined.

It could be said that there is a lot of room for improvement in performance for Cadmium Telluride based solar cells

3.2. Material Properties

Although there are many literatures about cadmium telluride, CdTe is not a well characterized material. The range of reported values for mobility and lifetime of carriers are huge and there are few reports on effective density of states, intrinsic carrier concentration, etc., which have a strong influence on the open circuit voltage. The material parameters are presented in Table 3.2.

Table 3.1 Survey of Measured CdTe Cells

window	Voc [V]	Jsc [mA/cm^2]	FF	Effi. [%]	Illumination	Ref.
CdS	0.725	21.23	0.67	10.31	AM1.5, 100 mW/cm^2	[7]
	0.7484	22.21	0.6339	10.5	AM1.5	[14]
	0.75	17	0.62	10.5	AM2 , 75 mW/cm^2	[52]
	0.754	27.9	0.61	12.8**	AM1.5 , 100 mW/cm^2	[29]
	0.612	20.5	0.605	8.7	ELH 87.5 mW/cm^2	[10]
	0.7	23.9	0.7	11	global 100 mW/cm^2	[55]
	0.78	22.5	0.58	11.6	87.3 mW/cm^2	[34]
	~0.5	~20	~0.5	~5**	AM1	[42]
	0.759	18.6	0.57	8.8	ELH white light	[30]
	~0.82	~ 21		~8	100 mW/cm^2	[8]
	0.783	24.98	0.627	12.3	AM1.5 global	[4]
	0.747	21.69	0.657	10.6	AM1.5 global	[17]
	0.747	17.3	0.67	8.7		[25]
	0.72	27.9	0.65	13.1	AM1 1000 W/m^2	[36]
	0.804	18.9	0.7	10.6	100 mW/cm^2	[56]
	0.68	20.5	0.56	7.9		[49]
	0.84	21.9	0.725	13.4	global 100 mW/cm^2	[47]
	0.79	26.2	0.615	12.7	global 100 mW/cm^2	[47]
	0.81	19.5	0.73	11.5	global 100 mW/cm^2	[47]
	0.715	24.2	0.60	10.3	global 100 mW/cm^2	[47]
	0.765	20.9	0.715	11.0	global 100 mW/cm^2	[47]
	0.797	21.1	0.672	11.3	AM1.5 100 mW/cm^2	[50]
ITO	0.81	20	0.55	10.5	85 mW/cm^2	[53]
	0.892	20.1	0.745	13.4* (14.4**)	AM1.5 100 mW/cm^2	[37]
TO	0.663	28.1	0.563	10.5	AM1.5 global 100 mW/cm^2	[32]
	0.82	21		10.7	AM1 106 mW/cm^2	[6]
	0.723	12	0.63	6	AM1	[31]

Table 3.1 continued

window	Voc [V]	Jsc [mA/cm^2]	FF	Effi. [%]	Illumination	Ref.
ZnO	0.45	18	0.41	4.8		[20]
thin film	0.48 ~					
single crys.	0.53	12.5		3.7	60.5 mW/cm^2	[51]
	0.54	19.5		7.6	100 mW/cm^2	
	0.54	19.5		8.8**	AM1 100 mW/cm^2	[5]
Au	0.807	20.9	0.67	15.1	AM2	[54]
$Zn_{0.3}Cd_{0.7}S$	0.78	23.4	0.594	10.84	ELH AM1	[16]

** Efficiencies with ** are the active area efficiencies.

* Efficiencies with * are the total efficiencies.

All the others do not specify which efficiency they were measuring.

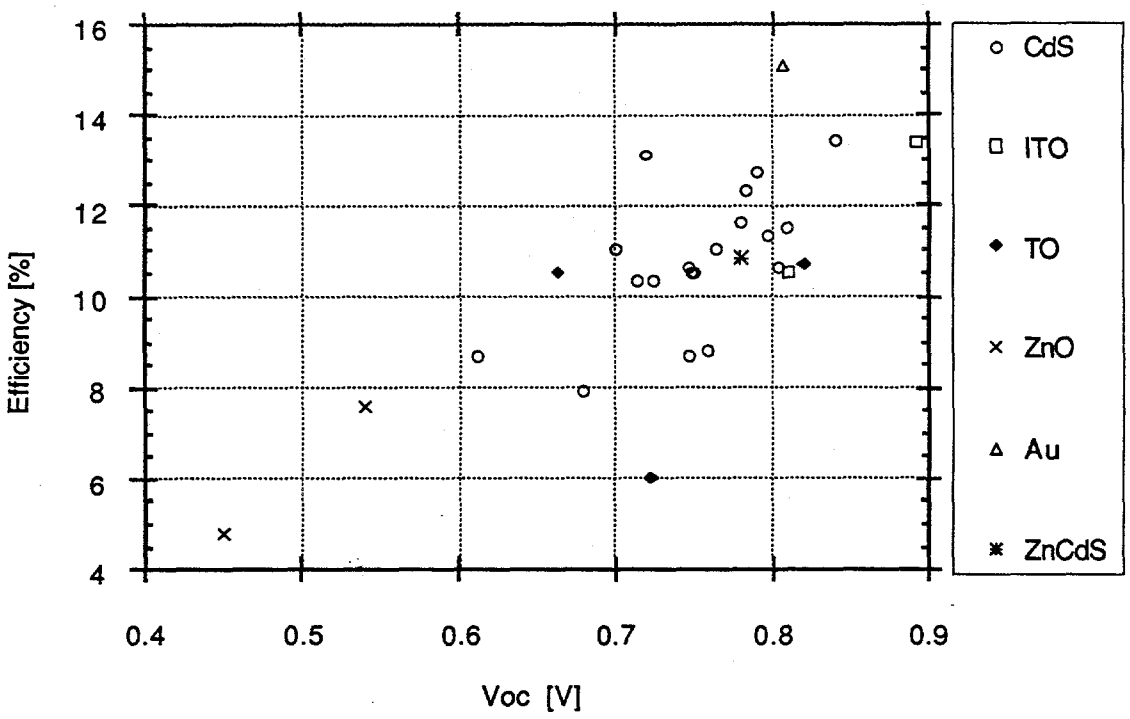

Figure 3.1 Open circuit voltage vs efficiency of surveyed CdTe solar cell performance. The symbols show which materials are used for window layers.

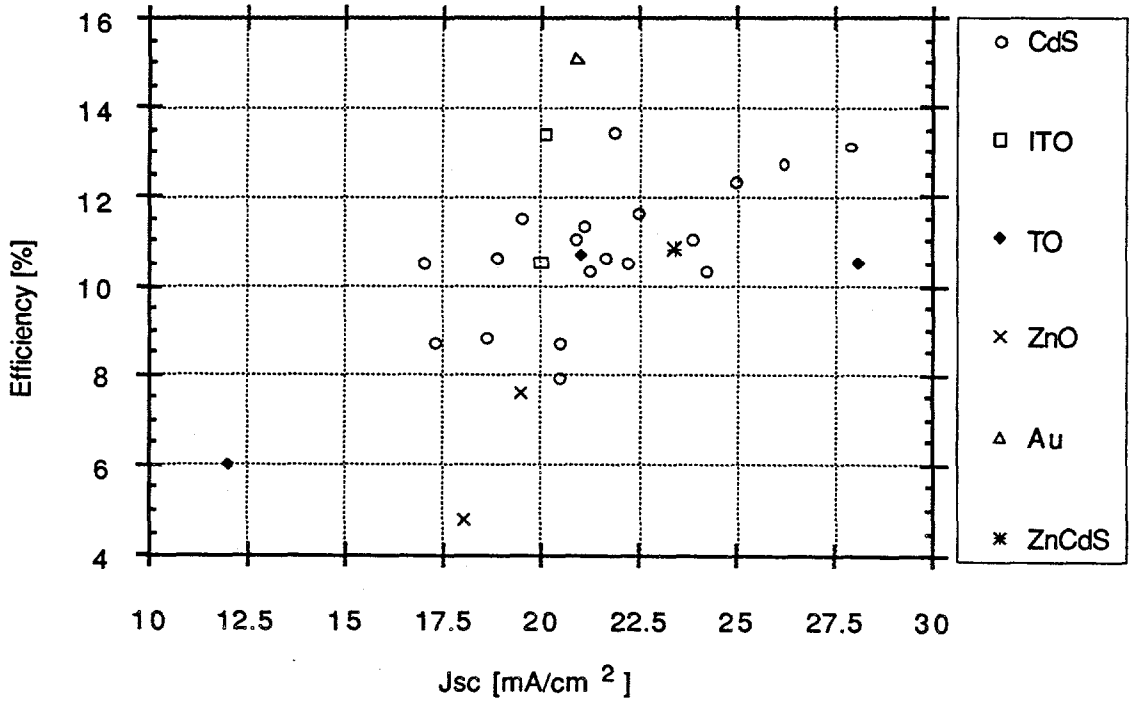

Figure 3.2 (a) Short circuit current vs efficiency of surveyed CdTe solar cell performance.

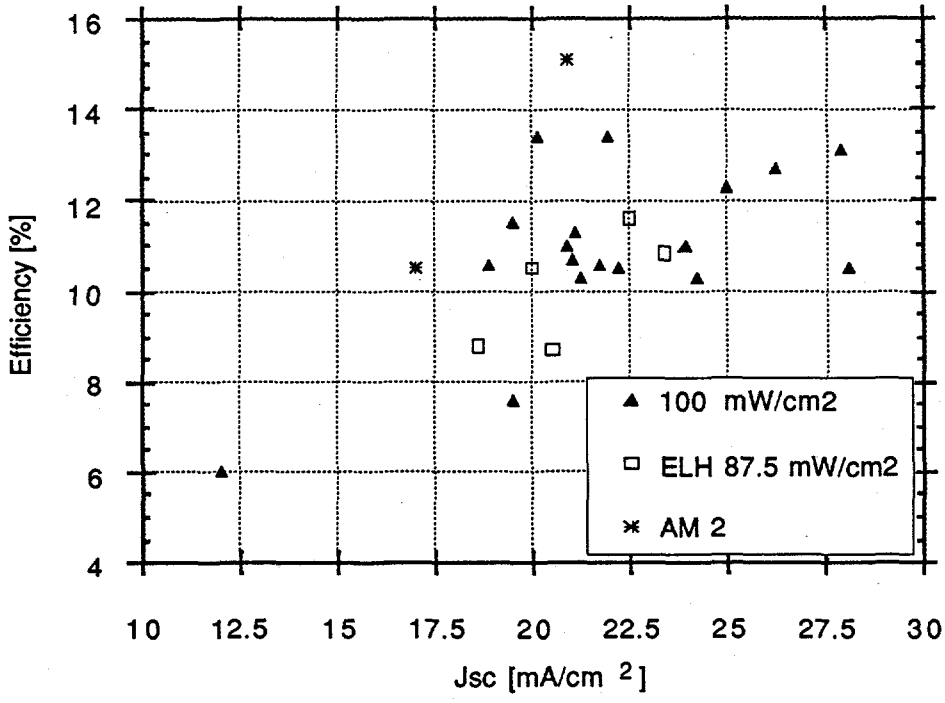

Figure 3.2 (b) Short circuit current vs efficiency of surveyed CdTe solar cell performance. The illumination intensity is indicated.

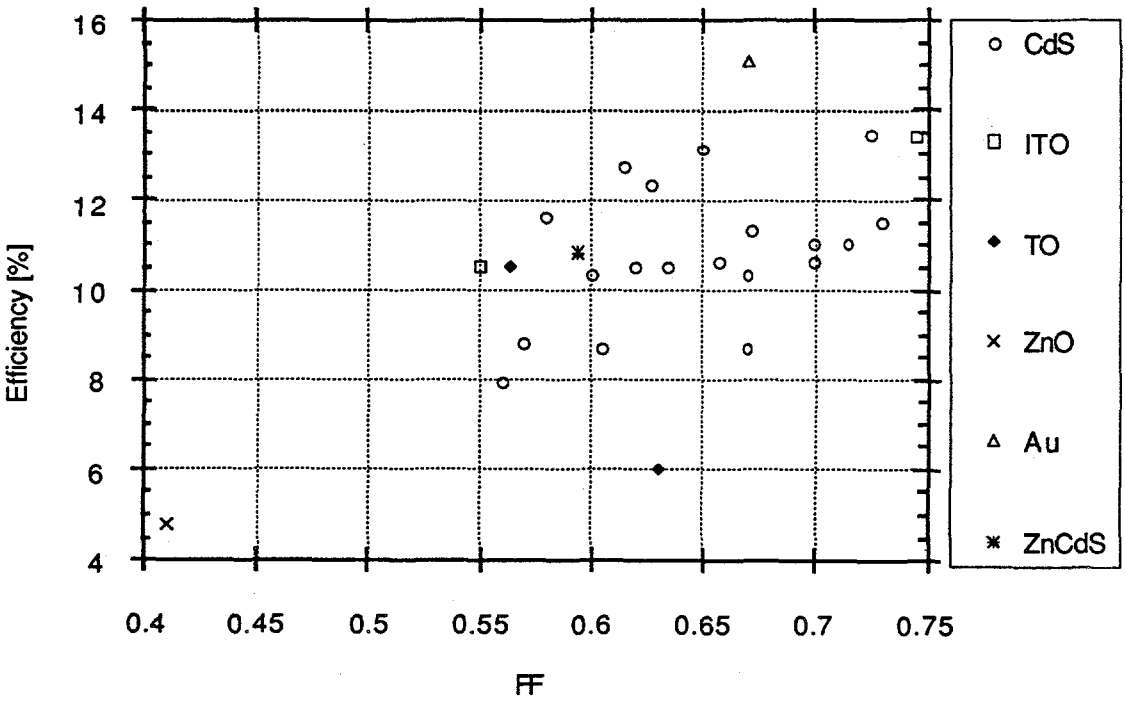

Figure 3.3 Fill factor vs efficiency of surveyed CdTe solar cells.

Table 3.2 CdTe Material Parameters

	values	references
Eg [eV]	1.51 (n - type) 1.46 (p - type)	[38]
	1.5	[10][9][15][26][42]
	1.45	[21][35][45][44][41]
	1.58	[13]
	1.44	[22][40][24][12]
	1.46	[28]
μ [$cm^2 V^{-1} s^{-1}$]	60 - 250 (n - type)	[47]
	5 - 10 (n- type)	[11]
	40 - 45 (p - type)	[10]
	65	[9]
	1200 at 170 K	[27]
	159 (p - type)	[28]
	800	[24]
	$\mu p = 60$, $\mu n = 600$	[43]
	40 - 60 (Hall)	[1]
	50 (Hall)	[2]
	4 (at the junction)	[46]
	$\mu n = 4$	[25]
a_o [nm]	0.647	[18]
	0.648+-0.002	[24]
mn*	(0.11+-0.01)mo	[27]
	0.1 mo	[46]
mh*	0.12 mo	[19]
	0.4 mo	[46]
ni [/cm^3]	1.0e7	[40]
Nc [/cm^3]	8.65e17	[24]
Nv [/cm^3]	1.27e19	[23]

Table 3.2 continued

	values	references
dielectric constant	7.21	[22]
	10.31 (static) 7.6 (optical)	[27]
	9.6	[24]
electron affinity [eV]	4.28	[40][16]
t [nsec]	6.7 for calculations, tn = 160, tp = 0.8	[9]
	100	[1]
	0.06	[33]
SI [cm/sec]	2.0e6	[33][23]

3.3. List of References for CdTe

1. N. V. Agrinskaya, and E. N. Arkadeva, "Fermi Level Pinning in the Middle of the Band Gap in CdTe: Ci Crystals: Role of Deep Localized States," Nuclear Instruments and Methods in Physics Research, Vol.A283, pp.260-262, 1989.

2. N. V. Agrinskaya, and O. A. Matveev, "On the Close Compensation Mechanism in CdTe(Li, Cl) Crystals," Nuclear Instruments and Methods in Physics Research, Vol.A283, pp.263-264, 1989.

3. S. P. Albright, B. Ackerman, and J. F. Jordan, "Efficient CdTe/CdS Solar Cells and Modules by Spray Processing," IEEE Transactions on Electron Devices, Vol.37, no.2, p.434, 1990.

4. S. P. Albright, J. F. Jordan, B. Ackerman, and R. R. Chamberlin, "Developments on CdS/CdTe Photovoltaic Panels at Photon Energy, Inc.," Solar Cells, Vol.27, pp.77-90, 1989.

5. J. A. Aranovich, D. Golmayo, A. L. Fahrenbruch, and R. H. Bube, "Photovoltaic Properties of ZnO/CdTe Heterojunction Prepared by Spray Pyrolsis," Journal of Applied Physics, Vol.51, no.8, 1980.

6. M. Barbe, F. Bailly, D. Lincot, and G. Cohen-Solal, "13% Conversion Efficiency in Cadmium Telluride Shallow Homojunction Solar Cell. Effects of Temperature and Intensity," 16th IEEE Photovoltaic Specialists Conference, p.1133, 1982.

7. B. M. Basol, "Electrodeposited CdTe and HgCdTe Solar Cells," Solar Cells, Vol.23, pp.69-88, 1988.
8. B. M. Basol, E. S. Tseng, R. L. Rod, S. Ou, and O. M. Stafsudd, "Ultra-Thin Electrodeposited CdS/CdTe Heterojunction with 8% Efficiency," 16th IEEE Photovoltaic Specialists Conference, p.805, 1982.
9. H. G. Bhimnathwala, N. R. Taskar, W. I. Lee, I. Bhat, S. K. Ghandhi, and J. M. Borrego, "Photovoltaic Properties of CdTe Layers Grown by OMVPE," 19th IEEE Photovoltaic Specialists Conference, p.1476, 1987.
10. R. W. Birkmire, B. E. McCandless, and W. N. Shafarman, "CdTe/CdS Solar Cells with Transparent Contacts," Solar Cells, Vol.23, pp.115-126, 1988.
11. R. H. Bube, "CdTe Junction Phenomena," Solar Cells, Vol.23, pp.1-17, 1988.
12. T. L. Chu, S. S. Chu, C. Ferekides, J. Britt, and C. W. Wu, "Thin Film CdTe Heterojunctions by MOCVD," 21st IEEE Photovoltaic Specialists Conference, p.777, 1990.
13. F. Abou-Elfotouh, D. J. Dunlavy, and H. S. Ullal, "Photoluminescence Studies of CdTe Polycrystalline Thin Films," Proceedings of the Polycrystalline Thin Film Program Meeting, p.71, 1989.
14. T. L. Chu, S. S. Chu, S. T. Ang, K. D. Han, Y. Z. Liu, K. Zweibel, and H. S. Ullal, "High Efficiency Thin Film Cadmium Telluride Solar Cells," 19th IEEE Photovoltaic Specialists Conference, p.1466, 1987.
15. T. L. Chu, S. S. Chu, S. T. Ang, and M. K. Mantravadi, "Thin Film Cadmium Telluride Solar Cells," Solar Cells, Vol.21, pp.73-80, 1987.
16. T. L. Chu, S. S. Chu, K. D. Han, Y. H. Liu, and M. K. Mantravadi, "Efficient Thin Film Cadmium Telluride Heterojunction Solar Cells," Solar Cells, Vol.24, pp.27-34, 1988.
17. T. L. Chu, S. S. Chu, K. D. Han, and M. K. Mantravadi, "Mercury Telluride as an Ohmic Contact to Efficient Thin Film Cadmium Telluride Solar Cells," 20th IEEE Photovoltaic Specialists Conference, p.1422, 1988.
18. S. H. Wei, L. G. Ferreira, and A. Zunger, "First-Principles Phase Diagram Calculation of 2-6 Semiconductor Alloys," Proceedings of the Polycristalline Thin Film Program Meeting, p.61, 1989.
19. A. L. Fahrenbruch, "Ohmic Contacts and Doping of CdTe," Solar Cells, Vol.21, pp.399-412, 1987.
20. M. Ginting, and J. D. Leslie, "Preparation and Electrical Properties of Heterojunction of ZnO on Zn3P2 and CdTe," Canadian Journal of Physics, Vol.67, p.448, 1989.

21. R. B. Gore, and R. K. Pandey, "Investigation of Deposition Parameters for the Non-Aqueous Electroplating of CdTe Films and Application in Electrochemical Photovoltaic Cells," Solar Energy Materials, Vol.18, pp.159-169, 1989.
22. R. D. Gould, and C. J. Bowler, "D.C. Electrical Properties of Evaporated Thin Films of CdTe," Thin Solid Films, Vol.164, pp.281-287, 1988.
23. L. C. Isett, "Photocapacitance and Current Collection in CdS/CdTe Thin-Film Solar Cells," IEEE Transactions on Electron Devices, Vol.ED-31, no.5, p.664, 1984.
24. B. B. Ismail, and R. D. Gould, "Structural and Electronic Properties of Evaporated Thin Filmd of Cadmium Telluride," Physica Status Solidi (a), Vol.115, p.237, 1989.
25. J. F. Jordan, and S. P. Albright, "Large-Area CdS/CdTe Photovoltaic Cells," Solar Cells, Vol.23, pp.107-113, 1988.
26. Y. Kawai, Y. Ema, and T. Hayashi, "Formation and Properties and Vacuum-Evaporated High Conductivity n-Type CdTe Films," Thin Solid Films, Vol.147, pp.75-81, 1987.
27. K. K. Kulshreshtha, P. K. Goyal, A. Pandya, and P. C. Mathur, "D.C. Galvanomagnetic Properties in a Heavily Compensated single crystal of n-Type CdTe," Journal of Materials Science, Vol.21, pp.2315-2321, 1986.
28. K. C. Mandal,S. Basu, and D. N. Bose, "Surface-Modified CdTe PEC Solar Cells," Solar Cells, Vol.18, pp.25-30, 1986.
29. H. Mutsumoto, K. Kuribayashi, H. Uda, Y. Komatsu, A. Nakano, and S. Ikegami, "Screen-Printed CdS/CdTe Solar Cell of 12.8% Efficiency for an Active Area of 0.78 cm^2," Solar Cells, Vol.11, pp.367-373, 1984.
30. P. V. Meyers, "Polycrystalline Cadmium Telluride n-i-p Solar Cell," SERI Annual Subcontract Report, 1989.
31. J. Mimila-Arroyo, Y. Marfaing, G. Cohen-Solal, and R. Triboulet, "Electric and Photovoltaic Properties of CdTe pn Homojunctions," Solar Energy Materials, Vol.1, pp.171-180, 1979.
32. K. W. Mitchell, C. Eberspacher, F. Cohen, J. Avery, G. Duran, and W. Bottenberg, "Process Towards High Efficiency Thin Film cdTe Solar Cells," Solar Cells, Vol.23, pp.49-57, 1988.
33. K. W. Mitchell, A. L. Fahrenbruch, and R. H. Bube, "Evaluation of the CdS/CdTe Heterojunction Solar Cell," Journal of Applied Physics, Vol.48, p.4365, 1977.
34. J. T. Moon, K. C. Park, and H. B. Im, "Photovoltaic Properties of CdS/CdTe Solar Cells Sintered with CdCl2," Solar Energy Materials, Vol.18, pp.53-60, 1988.
35. J. Morimoto, M. Fundamoto, S. Tashiro, M. Arai, T. Miyakawa, and R. Bube, "Spectral Analysis of Deep Centers in CdTe Single Crystals," Japaness Journal of Applied Physics,Vol.27, pp.2256-2259, 1988.

36. G. C. Morris, P. G. Tanner, and A. Tottszer, "Towards High Efficiency Electrodeposited CdS/CdTe Thin Film Cells," 21st IEEE Photovoltaic Specialists Conference, P.575, 1990.

37. T. Nakazawa, K. Takamizawa, and K. Ito, "High Efficiency Indium Oxide/Cadmium Telluride Solar Cells," Applied Physics Letters, Vol.50, p.279, 1987.

38. S. S. Ou, and O. M. Stafsudd, "Optical Properties of Electrochemically Deposited CdTe Films," Journal of Applied Physics, Vol.55, no.10, p.3769, 1984.

39. V. Ramanathan, L. Russell, C. H. Liu, and P. V. Meyers, "Characterization of CdTe Thin Film Solar Cells," 20th IEEE Photovoltaic Specialists Conference, p.1417, 1988.

40. D. T. Rasulov, "Research on the Photoelectrical Properties of pCdTe-nCdTe-nCdSe Film Structures"," Geliotekhnika, Vol.21, p.16, 1985.

41. A. Rohatgi, S. A. Ringel, R. sudharsanan, P. V. Meyers, C. H. Liu, and V. Ramanathan, "Investigation of Polycrystalline CdZnTe, CdMnTe, and CdTe Films for Photovoltaic Applications," Solar Cells, Vol.27, pp.219-230, 1989.

42. N. Romeo, A. Bosio, V. Canevari, C. Spaggiari, and L. Zini, "P-type CdTe Thin Films Doped During Growth by Neutral High Energy Nitrogen Atoms," Solar Cells, Vol.26, pp.189-195, 1989.

43. J. Rosenzweig, M. Adolf, H. Dignus, and U. Birkholz, "Characterization of High Resistivity CdTe Using Acoustoelectric Methods," Nuclear instruments and Methods in Physics Rearch, Vol.A283, p.255, 1989.

44. S. Saha, U. Pal, A. K. Chaudhuri, V. V. Rao, and H. D. Banerjee, "Optical Properties of CdTe Thin Films," Physica Status Solidi (a), Vol.114, p.721, 1989.

45. S. K. Sharma, and R. S. Srivastava, ""Anomalous Photovoltaic Effect in Vacuum-Deposited CdTe Films," Thin Solid Films, Vol.150, pp.217-226, 1987.

46. V. P. Singh, R. H. Kenney, J. C. McClure, S. P. Albright, B. Ackerman, and J. F. Jordan, "Electronic Characteristics of the Thin Film CdS-CdTe Photovoltaic Cells," 19th IEEE Photovoltaic Specialists Conference, p.216, 1987.

47. J. R. Sites, "Role of Polycrystallinity in CdTe and $CuInSe_2$ Photovoltaic Cells," SERI Annual Report, 1991.

48. H. Sitter, H. Heinrich, K. Lischka, and A. -Lopez-Otero, "Characterization and Annealing Behavior of Deep Levels in CdTe Epitaxial Layers," Journal of Applied physics, Vol.53, no.7, p.4948, 1982.

49. R. Sudharsanan, and A. Rohatgi, "Effect of Pre-Heat Treatment of CdS on MOCVD CdTe/CdS Solar Cell Performance," 21st IEEE Photovoltaic Specialists Conference, p.504, 1990.

50. N. Suyama, T. Arita, Y. Nishiyama, N. Ueno, S. Kitamura, and M. Murozono, "CdS/CdTe Solar Cells by the Screen-Printing-Sintering Technique," 21st IEEE Photovoltaic Specialists Conference, p.498, 1990.

51. M. S. Tomar, "Photovoltaic Properties of ZnO/p-CdTe Thin Film Heterojunctions," Thin Solid Films, Vol.164, pp.295-299, 1988.

52. Y. S. Tyan, and E. A. Perez-Albuerne, "Efficient Thin-Film CdS/CdTe Solar Cells," 16th IEEE Photovoltaic Specialists Conference, p.794, 1982.

53. J. G. Werthen, T. C. Anthony, A. L. Faherenbruch, and R. H. Bube, "A 10% Efficient ITO-CdTe heterojunction Solar Cell," 16th IEEE Photovoltaic Specialists Conference, p.1138,1982.

54. P. K. Raychaudhuri, "High Efficiency Au/CdTe Photovoltaic Cells," Journal of Applied Physics, Vol.62, no.7, p.3025, 1987.

55. P. V. Meyers, R. Liu, V. Ramanathan, and L. Russell, "Polycrystalline CdTe n-i-p Solar Cell and Module Development," Proceedings of the Polycrystalline Thin Film Program Meeting, p.27, 1989.

56. S. P. Albright, V. P. Singh, and J. F. Jordan, "Junction Characteristics of CdS/CdTe Solar Cells," Solar Cells, Vol.24, pp," 43-56, 1988.

4. Numerical Models for Optical Absorption

4.1. ADEPT Absorption Model Description

Very accurate absorption coefficients can be generated in ADEPT by reading various coefficients from the input data.
Almost all the known equations for different kinds of absorption are existent in the code. ADEPT is capable of handling allowed direct transitions, forbidden direct transitions as well as phonon assisted transitions. Basically the absorption model is divided into two regions, above the band gap energy and below the band gap energy.

4.1.1. Band Gap Absorption

In some materials, it is possible to have more than one optical band gap energy.[1] Up to three optical band gap energies can be selected in the code. The fundamental optical band gap energy can be the same as electrical band gap energy. If this is the case, by setting EG.OPT= -1, EG.OPT defaults to electrical band gap energy, Eg.
The equation for the absorption coefficient is,

$$\alpha = \beta 0 + \beta 1*(E-Eg)^{0.5} + \beta 2/E*(E-Eg)^{1.5} + \beta 3/E*(E-Eg)^{2} + \beta 4*E*(E-Eg)^{2}$$

$$+ \alpha 1/E*(E-Eg)^{0.5} + \alpha 2/E*(E-Eg2)^{1.5} + \alpha 3/E*(E-Eg3)^{1.5}$$

where E is the energy, Eg is the fundamental optical band gap energy, Eg2 is the second and Eg3 is the third optical band gap energies.

4.1.2. Sub-Band Gap Absorption

In some cases, absorption below the fundamental band gap energy is significant. There are two choices for handling these situations. One can select either TAIL.OPT or PHONON.OPT.

When TAIL.OPT is chosen, the code assumes that absorption is exponentially decaying below Eg (see figure 4.1). There are α_c and ζ, which determine how strongly and quickly the absorption is decaying should be present in the input deck.

$$\alpha_{tail} = \alpha_c * \exp[-\zeta * (\lambda-\lambda_c)]$$

λ_c is the cutoff wavelength.

It should be noted that there is no relation between absorption coefficients for above and below the band gap energy. Each energy region is dealt separately. Therefore, when sub-band gap absorption occurs, it is possible to have absorption coefficient calculated from the equation for the energies above the band gap is smaller than the absorption coefficient obtained by using the above equation at Eg. In this case, in order to smooth out the absorption coefficient curve, cut-off energy for sub-band gap absorption is automatically found in the code by bisectional method.

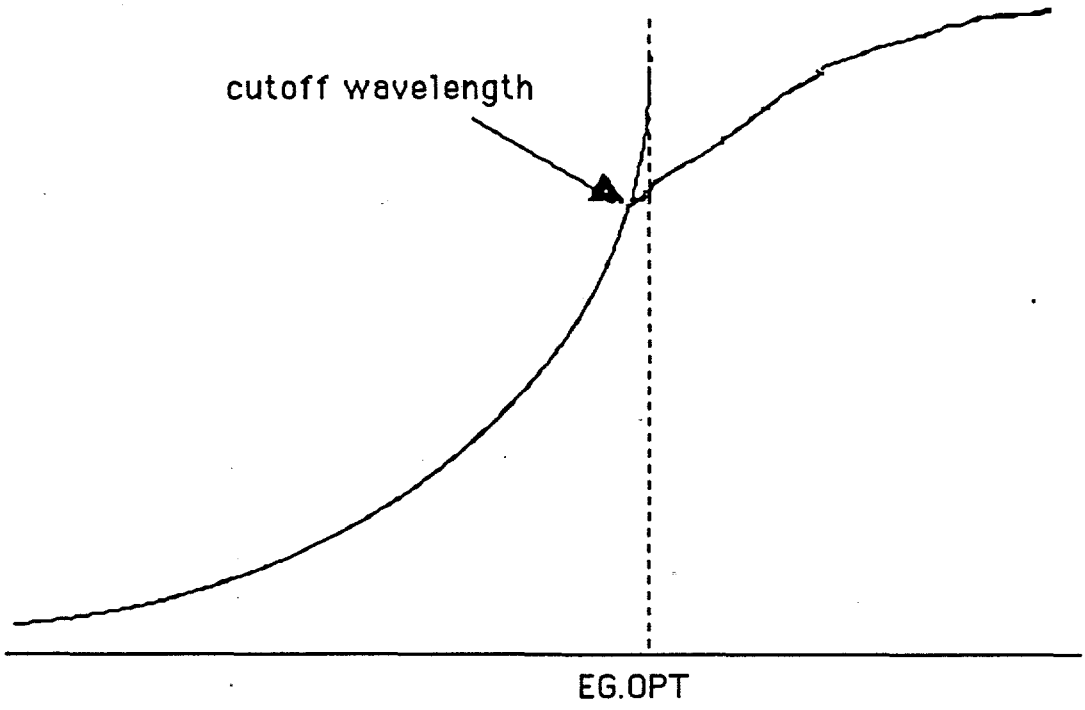

Figure 4.1 TAIL.OPT --- Residual absorption below the band gap energy is exponentially decaying.

It is wise to choose PHONON.OPT when the absorption coefficient varies significantly with the energy. This models phonon assisted transitions with up to 2 different phonon energies. The absorption coefficient due to phonon - assisted transition is given by

$$\alpha = \frac{B(h\nu - Eg + Ep)^2}{\exp(Ep/kT) - 1}$$

where B is a constant independent of phonon energy, Ep is the phonon energy and kT the thermal energy.

It has been reported that by extrapolating $\alpha^{1/2}$ vs energy curve to 0, regions of energies separated by intervals of phonon energies which are close to optical phonon wave number values were found.[1] Based on this fact, the code was modified to handle up to 5 sub regions below the band gap energy. These sub regions are separated by phonon energies (see figure 4.2). The user should enter the values of phonon energies, Ep1 and Ep 2 and the absorption coefficients at the edge of each sub region, α[i]. Inside each sub region, the absorption coefficient is generated assuming the residual absorption mechanism is due to phonon-assisted transitions.

In the i-th region, the absorption coefficient is calculated according to the following equation.

$$\alpha = \alpha[i] + \frac{b[i] \times (e - Eg + e[i])^2}{\exp(e[i]/kT) - 1}$$

where α[i] : known value (experimental value) of absorption coefficient at (Eg - e[1+i])

e[1] = Ep1
e[2] = Ep1+Ep2
e[3] = Ep1+Ep2+Ep1

Only Ep1, Ep2 and α[i] need to be defined by the user.

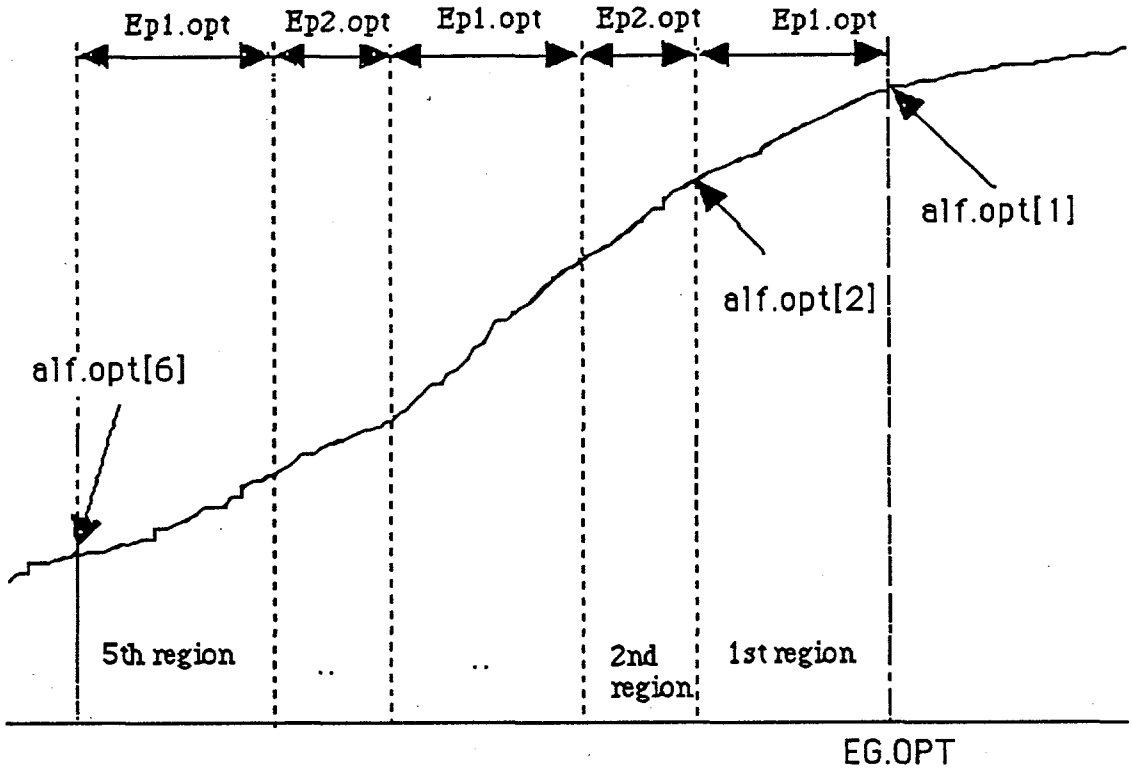

Figure 4.2 PHONON.OPT --- The sub-band gap absorption is due to phonon-assisted transitions.

In the code, above parameters are equivalent to the following:

equation	ADEPT	equation	ADEPT
b0	BO.OPT	Eg	EG.OPT
b1	B1.OPT	Eg2	EG2.OPT
b2	B2.OPT	Eg3	EG3.OPT
b3	B3.OPT	α_c	ALFC.OPT
b4	B4.OPT	ζ	ZETA.OPT
a1	A1.OPT	Ep1	EP1.OPT
a2	A2.OPT	Ep2	EP2.OPT
a3	A3.OPT	α[i]	ALF.OPT[i]

4.2. Absorption Models for Some Materials

4.2.1. $CuInSe_2$

The measured values of absorption coefficients were obtained from reference [2]. In figure 4.3, four absorption curves of $CuInSe_2$ with slightly different composition of Cu, In and Se are shown. Curve (a) and curve (c) correspond to Indium-rich $CuInSe_2$ while curve (b) is copper-rich CIS absorption curve. The absorption coefficients vs energy for stoichiometric $CuInSe_2$ is plotted and labelled curve (d). The absorption property is mostly studied in the stoichiometric $CuInSe_2$ which exhibits the best absorption property.

These curves with different composition of Cu, In and Se were all modelled using PHONON.OPT. The input data for the absorption entered into the code are presented in the following table 4.1. For all cases, PHONON.OPT are turned on by setting it to be TRUE and the phonon energies EP1.OPT and EP2.OPT are set to 31 and 19 mV respectively. All other parameters like optical band gaps ,etc. differ for each case. The absorption coefficients generated by ADEPT is plotted in figure 4.4. The dotted lines are the same curves as in figure 4.3 and the continues lines are numerically computed absorption coefficients according to the absorption models in ADEPT. Figure 4.4 (a) and figure 4.4 (c) shows the indium-rich or copper-poor $CuInSe_2$. The copper-poor CIS absorbs less above the band gap and also has less sub-band gap absorption. The value of fundamental optical band gap energy is slightly larger than others. Figure 4.4 (b) is the curve fit of copper-rich CIS. Fabricated solar cells usually have copper-rich regions near the back contact. Note that copper-rich CIS has much more residual absorption below the band gap energy than the others. The generated absorption coefficients of near-ideal stoichiometric $CuInSe_2$ is shown in figure 4.4 (d). It absorbs the photons most and it has been published that solar cells made with stoichiometric CIS have the best performances. [3]. The absorption study range was wide enough to determine the third optical band gap energy.

Table 4.1 Input data for $CuInSe_2$ absorption coefficients

	(a)	(b)	(c)	(d)
PHONON.OPT	TRUE			
EP1.OPT	0.031			
EP2.OPT	0.019			
EG.OPT	0.99	0.96	1.0	0.97
EG2.OPT	1.1	1.14	1.105	1.1
EG3.OPT	0	0	0	2.10
A1.OPT	2.890e4	5.099e4	5.200e4	5.270e4
A2.OPT	1.192e5	8.397e4	1.014e5	1.151e5
A3.OPT	0	0	0	4.518e5
ALF.OPT[1]	2.158e3	6.547e3	4.228e3	5.136e3
ALF.OPT[2]	1.438e3	5.191e3	1.733e3	2.420e3
ALF.OPT[3]	1.005e3	4.621e3	1.282e3	1.505e3
ALF.OPT[4]	0	3.882e3	0	1.027e3
ALF.OPT[5]	0	3.579e3	0	8.727e2
ALF.OPT[6]	0	3.185e3	0	7.417e2

All other unlisted inputs are defaulted to 0

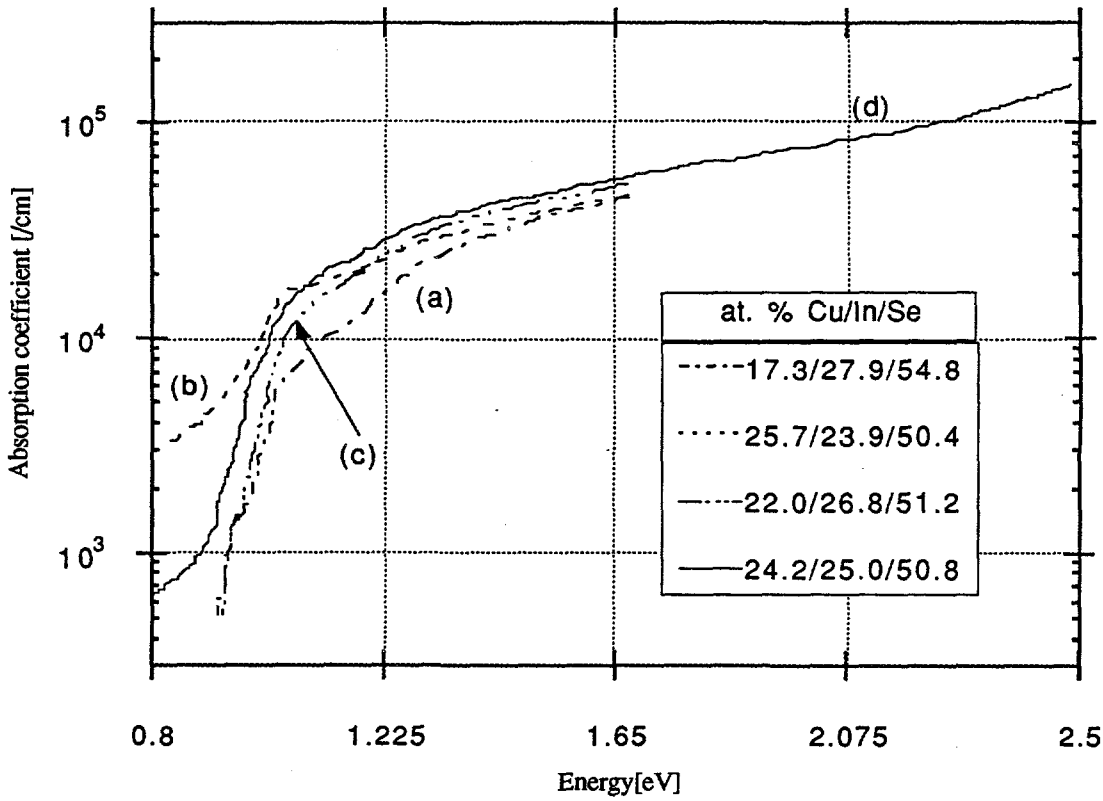

Figure 4.3 Absorption coefficients for different compositions of copper, indium and selenium. These data were obtained from reference [2].

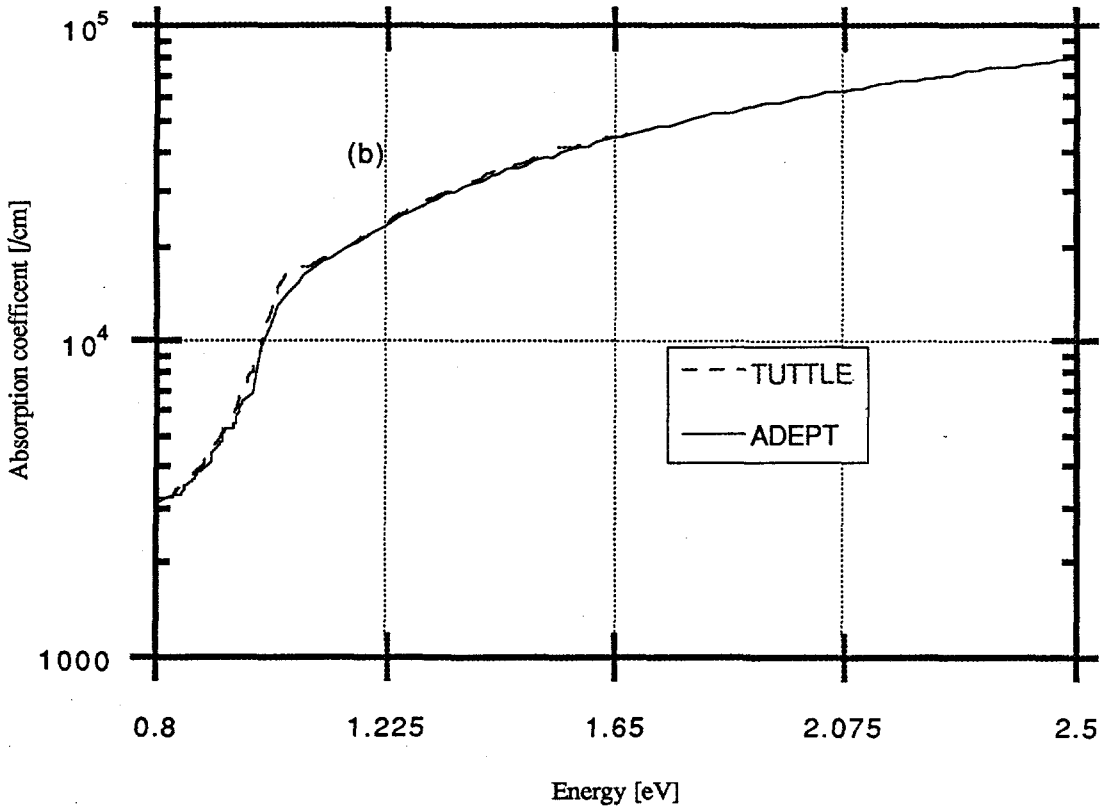

Figure 4.4(b) comparison of measured data and generated absorption coefficients by ADEPT of curve (b) in figure 4.3.

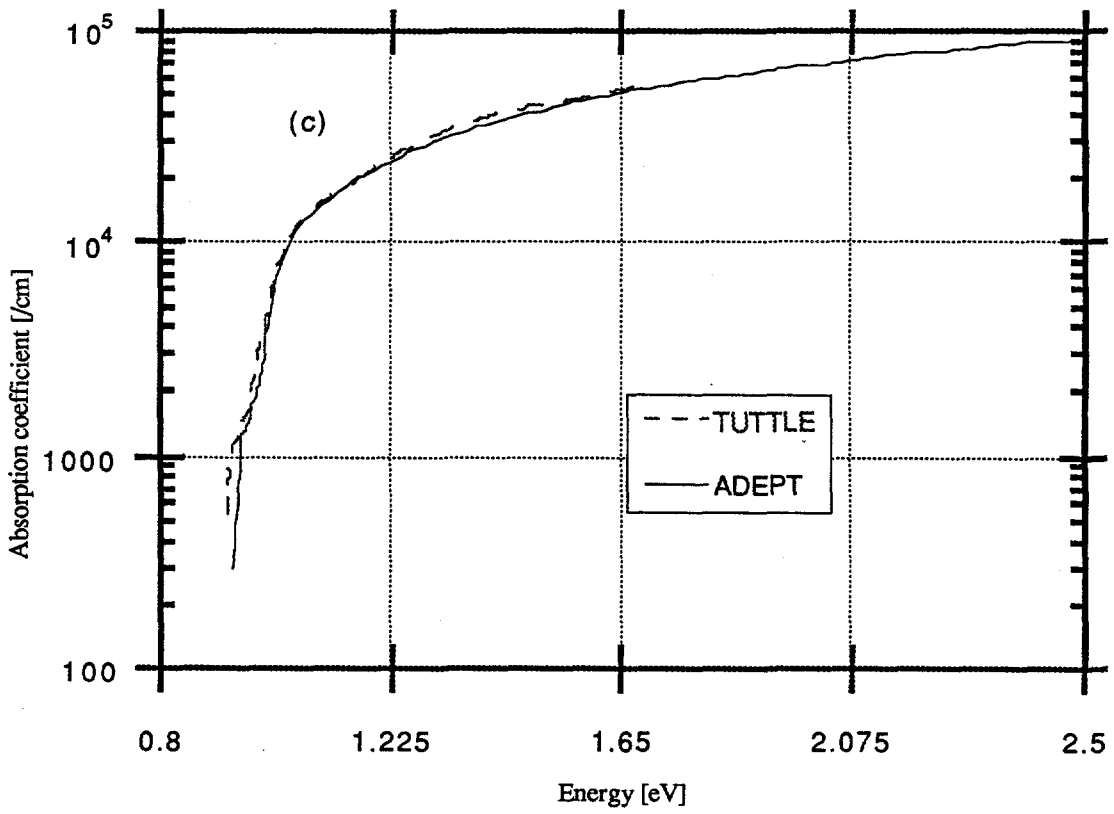

Figure 4.4(c) Comparison of measured and generated absorption coefficients by ADEPT of curve (c) in figure 4.3.

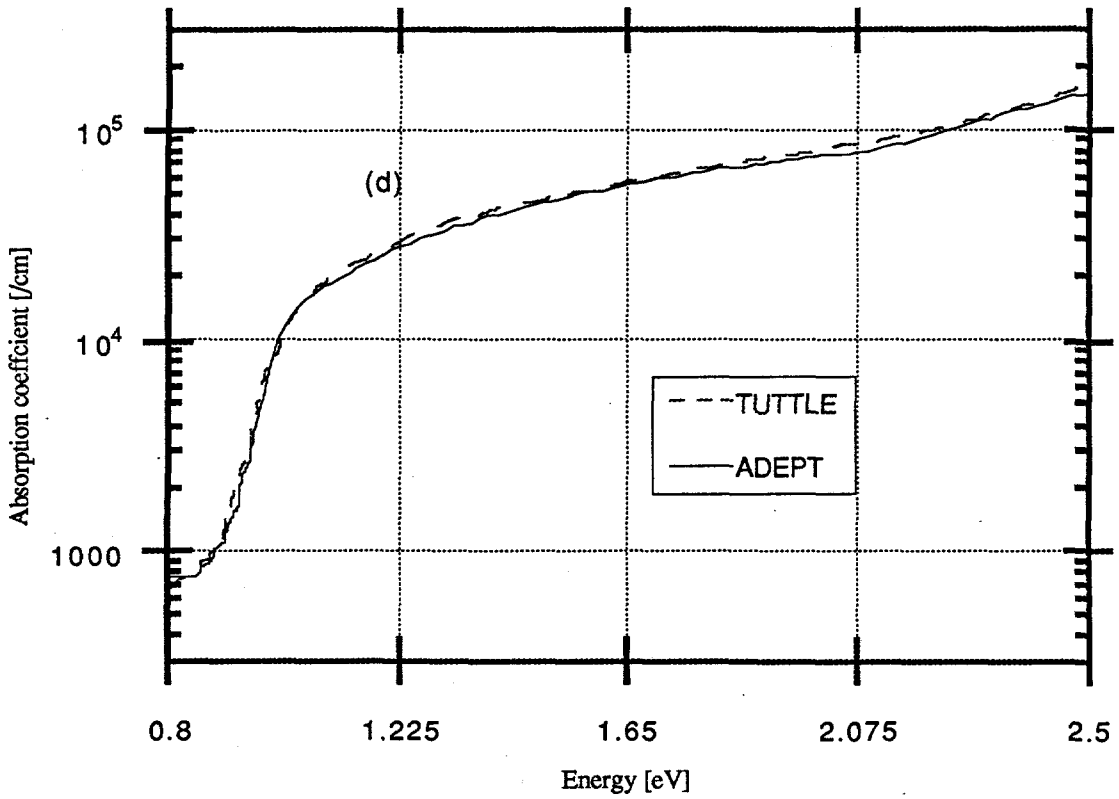

Figure 4.4 (d) Comparison of measured and generated absorption coefficients by ADEPT of curve (d) in figure 4.3. Notice that this curve is the absorption coefficients of the stoichiometric copper indium diselenide.

4.2.2. CdTe

For CdTe, the absorption properties are not studied in depth like CIS. However, it was possible to get absorption coefficients for n-type and p-type CdTe from the CdTe reference [4]. Since the residual absorption below the band gap energies does not vary significantly with the wavelength, TAIL.OPT is adequate enough to model the absorption. So for this case, TAIL.OPT is selected to be TRUE. The modeled absorption coefficients are shown in figure 4.5 (a) and 4.5 (b) as a function of wavelength. The dotted lines are the measured absorption curves and the continues lines are the numerically generated absorption curve by ADEPT. These figures show that p-type CdTe has smaller optical band gap and decays more faster below the band gap than n-type CdTe. The input data to ADEPT for generating the absorption coefficients of both p- and n-type CdTe ate represented in table 4.2.

Table 4.2 Input data for CdTe absorption coefficients

	p - CdTe	n - CdTe
EG.OPT	1.533	1.558
B0.OPT	0.8788e4	0.5898e4
B1.OPT	5.6555e4	6.0955e4
B2.OPT	-9.1585e4	-9.1585e4
B3.OPT	4.9434e4	4.9434e4
B4.OPT	1.4176e4	1.4176e4
TAIL.OPT	TRUE	
ALFC.OPT	1.14e4	1.204e4
ZETA.OPT	33	26.557

All other inputs are zero.

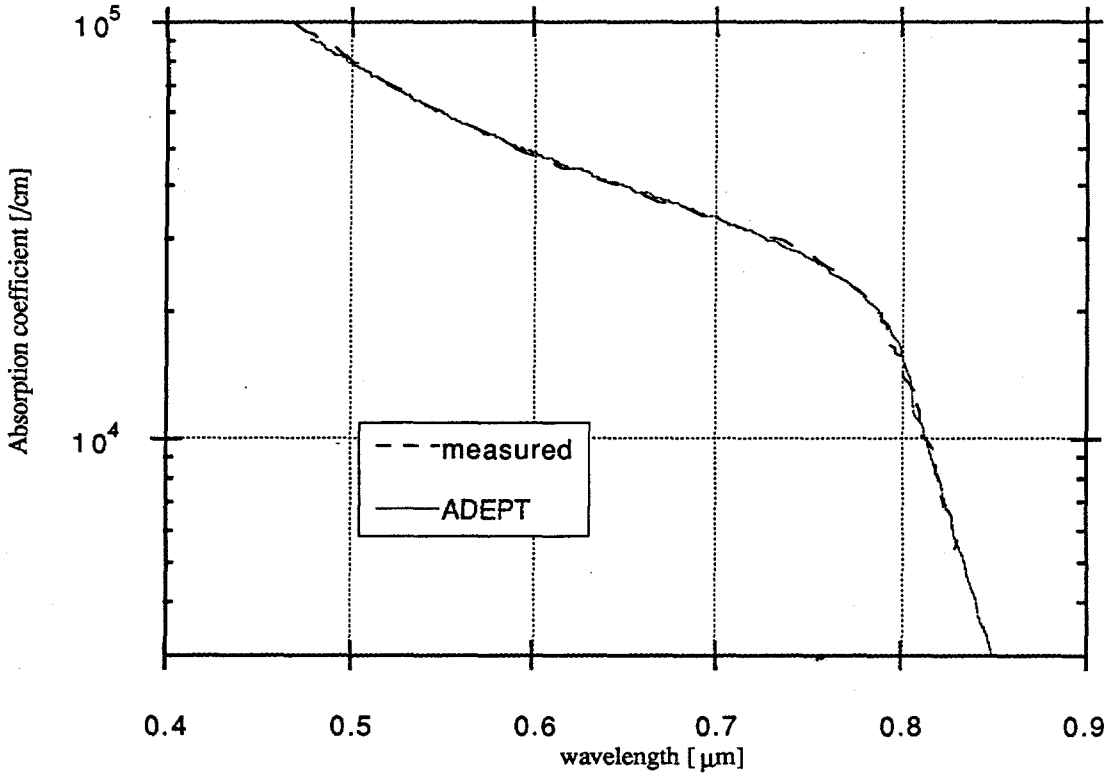

Figure 4.5 (a) This plot shows the experimentally measured absorption coefficients form reference [38] and fitted absorption curve by ADEPT of p - type CdTe.

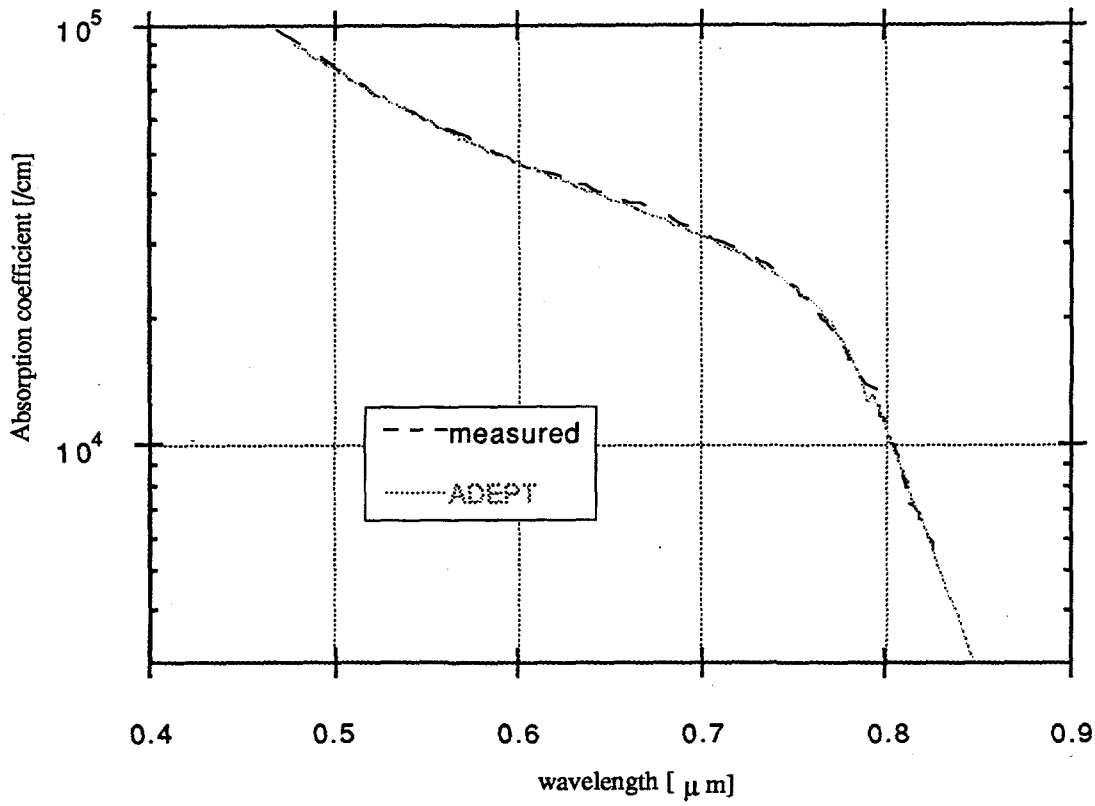

Figure 4.5 (b) Comparison of measured and generated absorption coefficients by ADEPT of n - type CdTe.

4.3. List of References for Optical Absorption

1. C. Rincon, C. Bellabarba, J. Gonzalez, and G. S. Perez, "Optical Properties and Characterization of CuInSe2," Solar Cells, Vol.16, pp.335-349, 1986.

2. J. R. Tuttle, R. Noufi, R. G. Dhere, C. Kennedy, R. Matson, J. Dolan, J. goral, "Optical Properties of CuInSe2 Thin Films," SERI Polycrystalline Thin Film Program Meeting, 1987.

3. J. R. Tuttle, M. Ruth, D. Albin, A. Matson, and R. Noufi, "Experiments on the Modification of the Bi-Layer Structure in CdS/CuInSe2 Devices," 20th IEEE Photovoltaic Specialists Conference, p.1525, 1988.

4. S. S. Ou, and O. M. Stafsudd," Optical Properties of Electrochemically Deposited CdTe Films," Journal of Applied Physics, Vol.55, no.10, p.3769, 1984.

Document Control Page	1. NREL Report No. NREL/TP-413-4835	2. NTIS Accession No. DE92001242	3. Recipient's Accession No.

4. Title and Subtitle

Development of a Computer Model for Polycrystalline Thin-Film $CuInSe_2$ and CdTe Solar Cells

5. Publication Date

April 1992

6.

7. Author(s)

J. L. Gray, R. J. Schwartz, Y. J. Lee

8. Performing Organization Rept. No.

9. Performing Organization Name and Address

Purdue University
School of Electrical Engineering
West Lafayette, IN 47907

10. Project/Task/Work Unit No.

PV231101

11. Contract (C) or Grant (G) No.

(C) XN-0-10013-1

(G)

12. Sponsoring Organization Name and Address

National Renewable Energy Laboratory
1617 Cole Blvd.
Golden, CO 80401-3393

13. Type of Report & Period Covered

Technical Report
1 January 1990 - 31 December 1990

14.

15. Supplementary Notes

NREL technical monitor: H. S. Ullal

16. Abstract (Limit: 200 words)

This report describes work to develop a highly accurate numerical model for $CuInSe_2$ and CdTe solar cells. ADEPT (A Device Emulation Program and Toolbox), a one-dimensional semiconductor device simulation code developed at Purdue University, was used as the basis of this model. An additional objective was to use ADEPT to analyze the performance of existing and proposed $CuInSe_2$ and CdTe solar cell structures. The work is being performed in two phases. The first phase involved collecting device performance parameters, cell structure information, and material parameters. This information was used to construct the basic models to simulate $CuInSe_2$ and CdTe solar cells. This report is a tabulation of information gathered during the first phase of this project on the performance of existing $CuInSe_2$ and CdTe solar cells, the material properties of $CuInSe_2$, CdTe, and CdS, and the optical absorption properties of $CuInSe_2$, CdTe, and CdS. The second phase will entail further development and the release of a version of ADEPT tailored to $CuInSe_2$ and CdTe solar cells that can be run on a personal computer. In addition, ADEPT will be used to analyze the performance of existing and proposed $CuInSe_2$ and CdTe solar cell structures.

17. Document Analysis

a. Descriptors

polycrystalline thin films ; thin films ; $CuInSe_2$; CdTe ; photovoltaics ; solar cells ; computer models ; numerical model

b. Identifiers/Open-Ended Terms

c. UC Categories

273

18. Availability Statement

National Technical Information Service
U.S. Department of Commerce
5285 Port Royal Road
Springfield, VA 22161

19. No. of Pages

41

20. Price

A03

Form No. 0069E (6-30-87)